Proceedings

Moisture sources for the explosive cyclogenesis of extratropical cyclone Miguel (2019) through a Lagrangian approach

Patricia Coll-Hidalgo[1,2], Albenis Pérez-Alarcón[1,3], José Carlos Fernández-Alvarez[1,3], Raquel Nieto[1] and Luis Gimeno[1]

[1] Centro de Investigación Mariña, Universidade de Vigo, Environmental Physics Laboratory (EPhysLab), Campus As Lagoas s/n, Ourense, 32004, Spain; patricia.coll@uvigo.es (P.C.-H.); albenis.perez.alarcon@uvigo.es (A.P.-A); jose.carlos.fernandez.alvarez@uvigo.es (J.C.F.-A); rnieto@uvigo.es (R.N.); l.gimeno@uvigo.es (L.G.)

[2] Empresa Cubana de Navegación Aérea, 10400 La Habana, Cuba

[3] Departamento de Meteorología, Instituto Superior de Tecnologías y Ciencias Aplicadas, Universidad de La Habana, 10400, La Habana, Cuba

* Correspondence: patricia.coll@uvigo.es (P.C.-H.)

Abstract: In this study, the moisture sources for the explosive cyclogenesis Miguel that occurred during 4-9 June 2019 in the North Atlantic were investigated. To determine the moisture sources, the Lagrangian FLEXPART particle dispersion model was used. The moisture uptake pattern revealed the western North Atlantic Ocean extending to north-western North America, the south-eastern coast of Greenland and the central North Atlantic Ocean around 45ºN and 50º-20ºW as the main moisture sources for Miguel explosive cyclogenesis. Furthermore, the moisture uptake from these regions was higher than the climatology. During the intensification of Miguel, the moisture contribution from oceanic sources was higher than terrestrial sources. Although the total amount of atmospheric moisture achieved during the explosive intensification was similar to that absorbed the 24 hours prior, they changed in intensity geographically, being more intense the local support over central and northern North Atlantic basin.

Keywords: extratropical cyclones, moisture sources, Lagrangian approach.

1. Introduction

Extratropical cyclones (ECs) are the synoptic phenomenon that typically cause severe weather in midlatitudes, including heavy rainfall and strong winds [1-6]. Chang et al. [7] showed that ECs play an important role in the poleward transport of heat and momentum. In the North Atlantic and Northern Europe, rainfall associated with cyclones account for 70-80 % of total precipitation [8].

ECs intensity and the amount of precipitation are linked to the processes of transport and distribution of moisture during their development phases [9]. Moreover, it has been accepted that the moisture transport intensity is significantly different at different times, mainly depending on the location and intensity of the cyclone [10]. About moisture transport mechanisms in ECs, Sodemann and Stohl [11], showed that individual cyclones were responsible for the formation and maintenance of atmospherics rivers (ARs). However, very long ARs require more than one cyclone to be maintained, before the moisture is released as precipitation [9]. Some studies consider that ARs are portions of the EC system [12-15]. Furthermore, Gimeno et al. [16] pointed out that ARs are associated with the pre-cold frontal region and the warm conveyor belt [17] of ECs.

ECs transport and distribution processes have been broadly discussed, as well as the origin of their moisture. Stohl and James [18] investigated an extreme precipitation event over Europe associated with an EC, identifying the Mediterranean Sea as the major evaporation source region of the water that became precipitation. These authors, also, identified that the trajectories of the particles involve in the EC describe pathways from North Africa, which gained moisture over Argelia and Mediterranean Sea. Dacre et

al. [15] used the water vapor budget of 200 ECs to determine that tropical moisture reaching the extratropics only contributes to mid-level moisture, above the boundary layer. Additionally, Zhao et al. [10], for a heavy snowstorm over northeastern China, caused by an EC featuring a back-bent warm front structure, found that the moisture mainly come from the middle and lower troposphere.

Specifically, in the Iberian Peninsula (IP), where 85% of recorded precipitation and wind extreme events are clearly associated with ECs [19], western IP coast are the areas most exposed to ECs [20]. According to the results in Hénin et al. [19], in this region the winter climatological is mostly driven by the North Atlantic flux and moisture transport. Moreover, Eiras-Barca et al. [21] studied an explosive cyclogenesis occurring in October 1987 northwest to the IP. The related AR event resulted in record winds of 100 km h^{-1} and daily precipitation of over 100 mm day^{-1} in Galicia (on the northwestern corner of the IP) and Portugal. The authors obtained for this event that more than 60 % of the resulting precipitation was a tropical origin.

To estimate moisture sources and sinks, several authors have been used extensively Lagrangian and Eulerian moisture tracking models. The Lagrangian technique is able to track the particle transport routes and moisture gain/loss along the trajectories; while, Eulerian ones has limitations to clarify the moisture sources and processes affecting moisture accumulation (see Gimeno et al. [22] and references therein). Lagrangian approach was widely applied to understand the hydrological cycle in more than a few regions around the world [e.g. 10, 18, 23-32].

In view of the origin of moisture in ECs is still an important discussion, the aim of this work is to investigate the moisture sources for the explosive cyclogenesis Miguel developed over the North Atlantic on 4-9 June 2019 through a Lagrangian backward trajectory technique. We have selected the EC Miguel as case of study due to its significant impact in the region [33], and the alarming projections of natural hazards attributed to these type of meteorological systems [34-37].

According with the Spanish Agency of Meteorology (AEMET, spanish acronym) [33], when Miguel moving towards to the east, in the North Atlantic, it underwent an explosive cyclogenesis near the Galicia coast. Later, Miguel moved quickly towards France and the British Isles. Finally, it continued moving to the northwest, until it reached Scandinavia, where it completed its life cycle. Among the ECs that have affected Europe in the May-June period from 1979 to 2019, Miguel is considered peculiar, because it exhibits an unusual explosive cyclogenesis, and, a very exceptional track record for this type of event during this period of the year [38].

2. Materials and Methods

2.1 Data

In this study was used the European Center for Medium-Range Weather Forecasts (ECMWF) ERA-5 reanalysis [39] and ERA-Interim reanalysis [40]. FLEXPART model [41] was forced by ERA-Interim data with horizontal grid spacing of 1° of latitude by longitude and 61 vertical levels, from 1000 to 0.1 hPa. From ERA-5 were extracted the geopotential height data at the constant pressure level of 1000 hPa (z1000), Vertically Integrated Moisture Flux divergence (VIMF) and the sea level pressure at every 6 hours (0000, 0600, 1200, and 1800 UTC), on a regular latitude longitude grid of 0.25° of horizontal resolution.

2.2 FLEXPART simulations

To investigate the moisture sources for EC Miguel, the outputs from the Lagrangian particle dispersion model FLEXPART v9.0 [41] were used from 0000 UTC 4 June to 1800 UTC 9 June. The global model simulates the trajectory of approximately 2.0 million particles homogeneously distributed in the atmosphere. Particles were then allowed to move freely with the winds for the duration of the simulation [18]. Model global outputs were obtained every 6-h on the initial grid resolution (1° x 1°).

2.2 Trajectory of the explosive cyclogenesis Miguel and characteristic

Using the University of Hamburg approach [42], the EC center was determined as local minima in the geopotential 1000hPa field. The radius from Miguel center was set to 400 km, according with the results of Pepler and Dowdly [43]. Figure 1 shows the trajectory of Miguel from 0000 UTC 5 June to 1800 UTC 9 June.
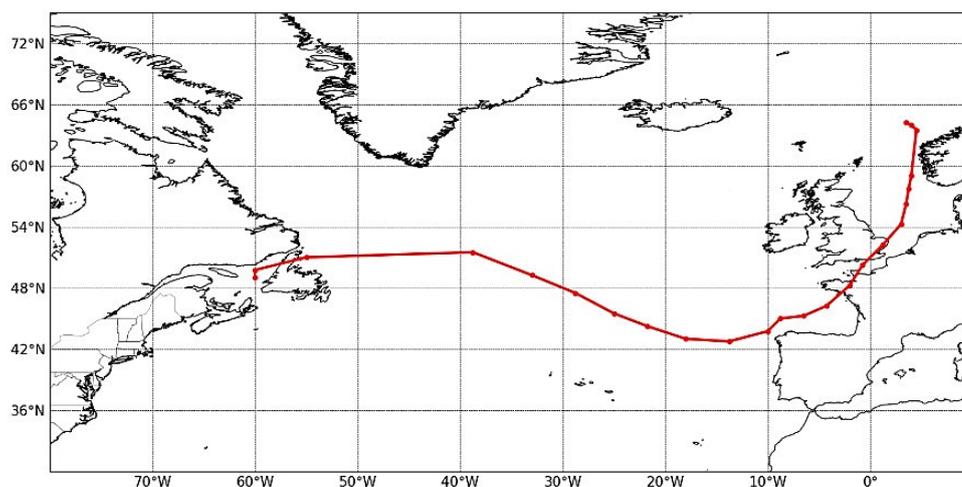
1 **Figure 1:** Trajectory of the extratropical cyclone Miguel (2019) estimated as the minimum z1000
2 from 0000 UTC 4 June to 1800 UTC 9 June.

3   To estimate the period of explosive cyclogenesis, the normalized deepening rate
4 (NDR) criterion of Sanders and Gyakum [44] was applied. These authors proposed a EC
5 as explosive cyclogenesis when the surface pressure drop in the center of the low is
6 higher than 24 hPa in 24 hours, at a normalized latitude of 60^0N, following Equation 1:

$$NDR = \frac{\Delta p}{24} \cdot \frac{\sin 60}{\sin \varphi} > 1 \, Bergeron \tag{1}$$

7 where Δp is the pressure drop in hPa in 24 hours; φ the mean latitude (in degrees) of the
8 center of the cyclone during the 24 hours period.
9   Figure 2 shows that the NDR exceeds, by first time, the limit value of 1 at 1200 UTC
10 on the 6th of June. It suggests that the explosive cyclogenesis started from 5 June at 1200
11 UTC, intensifying even more still 18 UTC 6 June, and it occurred over the North Atlantic
12 Ocean near northwest IP, as it is shown in Figure 3b. Naray [38] showed that the
13 intensification of Miguel was favored by the presence at low levels of a baroclinic region
14 and an intense AR. At high levels, atmospheric conditions were characterized by a local
15 intensification of the Jet Streak in western Europe, and a possible downstream
16 development caused by the existence of a quasi-stationary Rossby wave in the North
17 Atlantic.
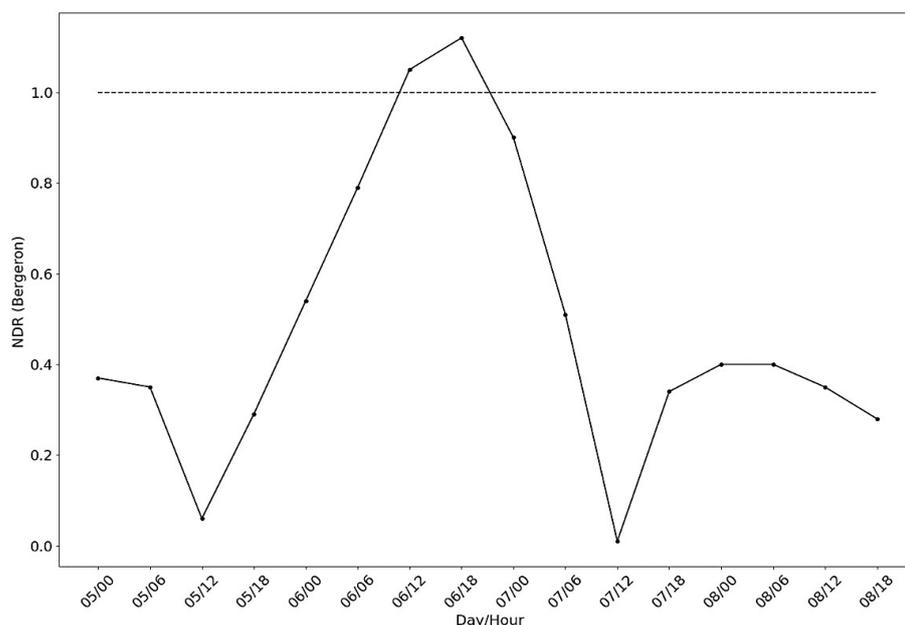
Figure 2: The normalized deepening rate (NDR) computed every 6 h during EC Miguel (2019) life cycle.

2.3 Lagrangian moisture budget diagnostic

Following Stohl and James [18], from the FLEXPART output, changes in specific humidity over time (dq/dt) were used to diagnose the moisture budget of a particle. The net rate of change of the water vapor content of a particle is estimated as:

$$e - p = m \frac{dq}{dt},$$ (2)

where $(e - p)$ represents the freshwater flux in the parcel.

The sum of all the $(e - p)$ values for all particles residing in a specific atmospheric column over an area A represents the surface freshwater flux over A. It was computed as:

$$E - P \approx \frac{\sum_{k=1}^{K} (e - p)}{A},$$ (3)

where E is the evaporation rate per unit area and P is the precipitation rate per unit area. It is possible to identify the regions where particles have either gained ($E - P > 0$) or lost ($E - P < 0$) moisture along their path towards the selected area. The enclosed area by the radius of each EC Miguel track position was selected as the target region for the analysis of their moisture sources. Thus, the particles within this contour were tracked backward in time up to 10 days, which is typically used in Lagrange approach as the estimated residence time of the water vapor in the atmosphere [45,46].

3. Results and Discussion

Figure 3a shows the moisture uptake 24 hours previous to the explosive cyclogenesis phase. The $E - P > 0$ field shows that the western North Atlantic Ocean (close to the Bahamas Archipelago), the south-eastern coast of Greenland, and the North Atlantic Ocean around 45ºN of latitude were the main moisture sources for the EC. Moreover, from the continental United States of America was identified a weak contribution. The moisture uptake from oceanic moisture sources (50.25%) is almost similar to terrestrial sources contribution (49.74%) in the 24 hours previous to Miguel explosive cyclogenesis. Nevertheless, during the intensification, the oceanic moisture contribution was 13% higher than terrestrial one. Moreover, the North Atlantic Subtropical High-Pressure system (NASH) circulation was identified as the moisture transport mechanism from the lower latitudes, as reinforced the VIMF for both periods, 24 hours previous explosive cyclogenesis (Figure 3a) and during the intensification (Figure 3b).

Furthermore, during the explosive cyclogenesis time, the moisture uptake composite pattern from 1200 UTC 5 June to 1200 UTC 6 June (Figure 3b), exhibited local evaporation and water vapor coming from the north near Greenland as stronger sources, although it is notable the moisture contribution from the southeast USA and the western North Atlantic. In general, the Lagrangian analysis suggests that a local intensification of moisture uptake is an important moisture source during this period. Similarly, Eiras-Barca et al. [21] suggested that the vast majority of the moisture in an extratropical explosive cyclogenesis occurred just off the coast of Galicia has its origin in the tropical regions and local sources occurring along the frontal region.
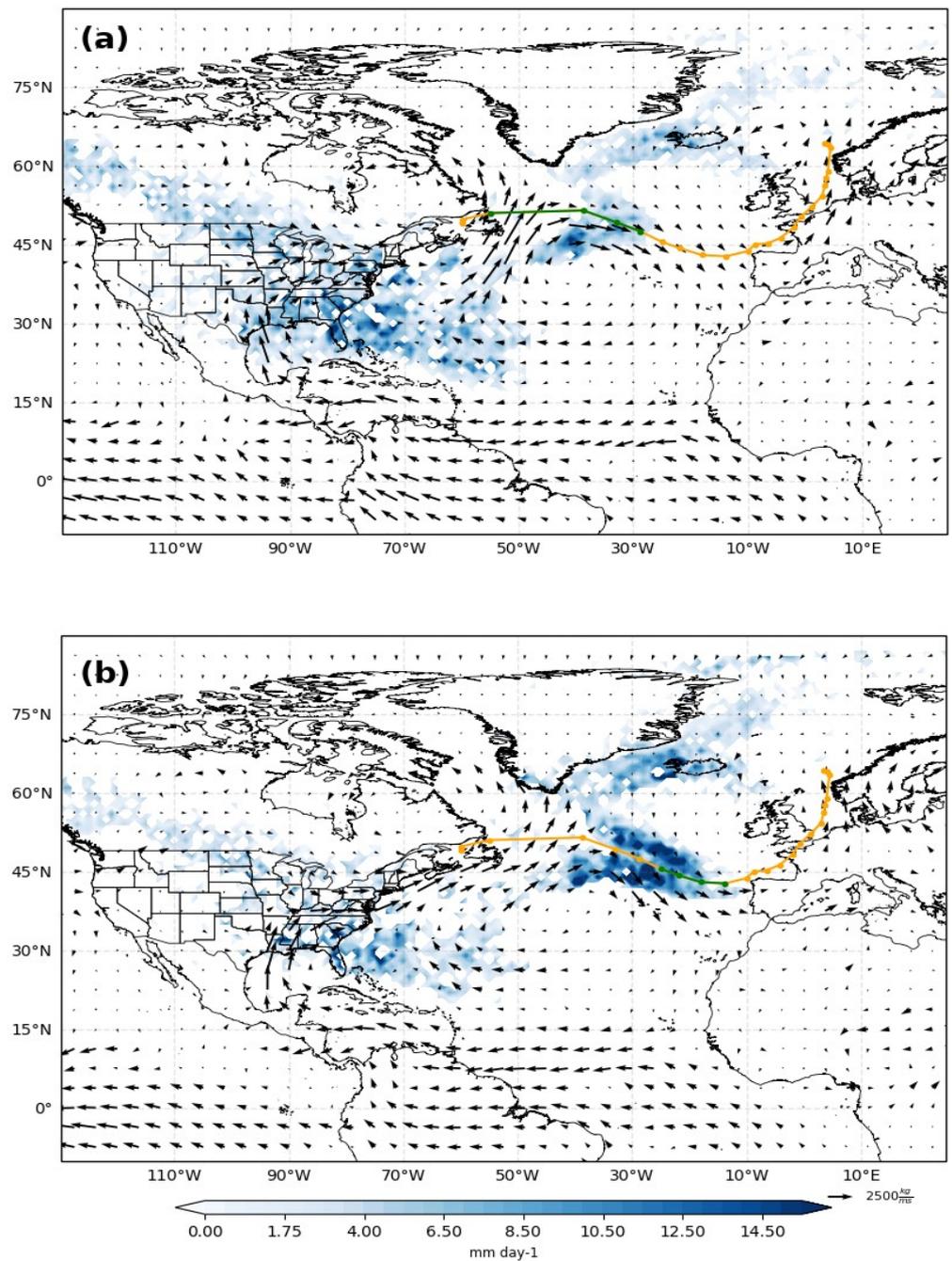
Figure 3: Composite of ($E - P$) > 0 (blues) during (a) 24 hours before EC Miguel explosive cyclogenesis, and (b) EC Miguel explosive cyclogenesis, from 1200 UTC 5 June to 1200 UTC 6 June. In arrows the vertical integrated moisture flux (VIMF) from ERA-5. The orange line denotes the complete Miguel trajectory and the green line represents the analyzed Miguel track.

Figure 4a shown moisture uptakes anomalies 24 hours before the explosive cyclogenesis. It is important to note that before intensification as well as during this process, was absorbed most atmospheric humidity than the climatological moisture uptake along Greenland coast, the western North Atlantic, the Gulf of Mexico and over continental North America.
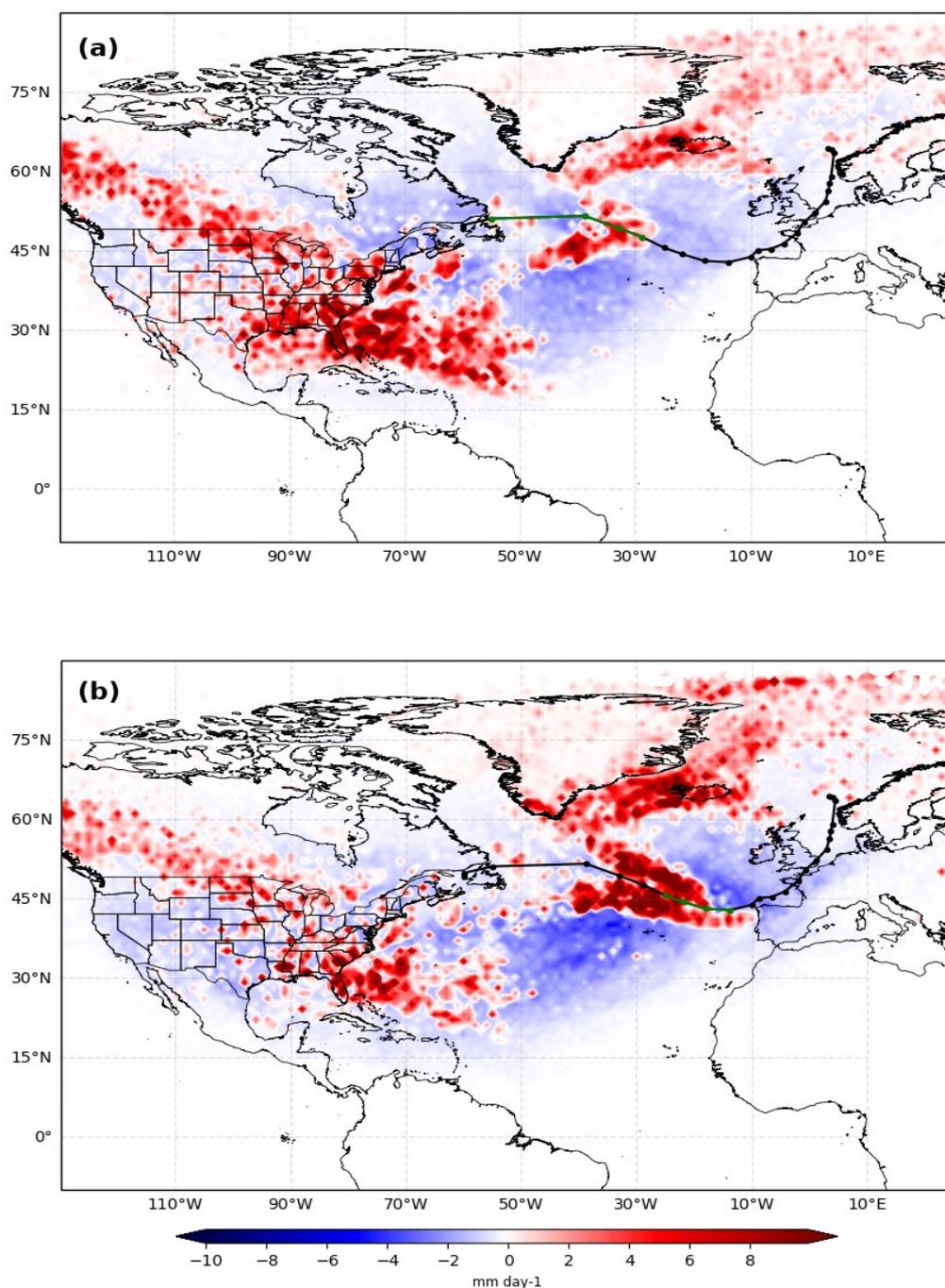
Figure 4: Moisture uptake anomalies for EC Miguel (a) 24 hours before the explosive cyclogenesis, and (b) during the explosive cyclogenesis, from 1200 UTC June 5th to 1200 UTC June 6th. The black line denotes the Miguel trajectory and the green line represents the analyzed Miguel Track.

During the intensification of Miguel (Figure 4b), an increase in positive moisture uptake anomalies is observed along the southeast coast of Greenland, in the Atlantic Ocean under Miguel circulation, and a decrease in positive moisture uptake anomalies in the western Atlantic, Gulf of Mexico and over North America. As it was commented before, according to Naray [38], the cyclone traveled through a jet stream crossing Greenland in a Northwest-Southeast direction. At the end of the intensification process Miguel was inside a trough at high levels. This trough was originated by the rupture of extensive cyclonic waves that caused the intensification of the jet stream and his

movement towards the Equator [38], probably starting a higher transport of moisture from the southeastern Greenland coast region.

4.Conclusions

In this study was investigated the moisture sources for the explosive cyclogenesis of the extratropical cyclone (EC) Miguel developed over North Atlantic on 4-9 June 2019, through a Lagrangian backward trajectory technique. From computing the normalized deeping rate (NDR) was identified that the explosive cyclogenesis occurred from 5 June at 1200 UTC to 6 June at 1200 UTC, but the intensification process continued still to 6 June at 1800 UTC. Moreover, we investigate moisture sources regions from the composite of $(E − P) > 0$ during EC Miguel explosive cyclogenesis and 24 hours before.

The Lagrangian analysis revealed that the western North Atlantic Ocean, close to the Bahamas Archipelago, the south-eastern coast of Greenland and the North Atlantic Ocean around 45ºN of latitude as the main moisture sources for Miguel development. Additionally, our results suggest that the local intensification region is an important moisture source during Miguel intensification. Furthermore, the positive moisture uptake anomalies in the southeast Greenland coasts during explosive cyclogenesis is notable, and, probably linked to the intensification of the jet stream and his movement towards the Equator. Furthermore, a distinctive feature during Miguel explosive cyclogenesis is the moisture contribution from oceanic sources.

5. Patents

Conflicts of Interest: The authors declare no conflict of interest.

References

1. Leckebusch, G.C.; Ulbrich, U. On the relationship between cyclones and extreme windstorm events over Europe under climate change. *Glob. Planet. Change* **2004**, 44, 181–193, doi: 10.1016/j.gloplacha.2004.06.011
2. Pfahl, S.; Wernli, H. Quantifying the relevance of cyclones for precipitation extremes. *J. Climate* **2012**, 25, 6770–6780, doi: 10.1175/JCLI-D-11-00705.1
3. Reale, M.; Lionello, P. Synoptic climatology of winter intense precipitation events along the Mediterranean coasts. *Nat. Hazards Earth Syst. Sci.* **2013**, 13, 1707-1722, doi: 10.5194/nhess-13-1707-2013
4. Pfahl, S. Characterising the relationship between weather extremes in Europe and synoptic circulation features. *Nat. Hazards Earth Syst. Sci.* **2014**, 14, 1461 –1475, doi: 10.5194/nhess-14-1461-2014
5. Raveh-Rubin, S.; Catto, J.L. Climatology and dynamics of the link between dry intrusions and cold fronts during winter, Part II: Front-centred perspective. *Clim. Dyn.* **2019**, 53, 1893 –1909, doi: 10.1007/s00382-019-04793-2
6. Dowdy, A.J.; Catto, J.L. Extreme weather caused by concurrent cyclone, front and thunderstorm occurrences. *Sci. Rep.* **2017**, 7, 40359, doi: 10.1038/srep40359
7. Chang, E.K.M.; Lee, S.; Swanson, K.L. Storm track dynamics. *J. Climate* **2002**, 15, 2163–2183, doi: 10.1175/1520-0442(2002)015,02163: STD.2.0.CO;2
8. Hawcroft, M. K.; Shaffrey, L. C.; Hodges, K. I.; Dacre, H. F. How much Northern Hemisphere precipitation is associated with extratropical cyclones? *Geophys. Res. Lett.* **2012**, 39, doi: 10.1029/2012GL053866
9. Ekrem, P.A. NAWDEX case study: Water vapor transport in atmospheric rivers and quantifying hand over of moisture between extratropical cyclones. Master Thesis, University of Bergen, Location of University, September 25th 2020.

10. Zhao, Y.; Fu, L.; Yag, Ch-F.; Chen, X-F. Case Study of a Heavy Snowstorm Associated with an Extratropical Cyclone Featuring a Back-Bent Warm Front Structure. *Atmos.* **2020**, 11, 1272, doi:10.3390/atmos11121272

11. Sodemann H.; Stohl, A. Moisture Origin and Meridional Transport in Atmospheric Rivers and Their Association with Multiple Cyclones. *Mon. Wea. Rev.* **2013**, 141, 2850–2868, doi: 10.1175/MWRD-12-00256.1

12. Ralph, F. M.; Neiman, P. J.; Wick, G. A. Satellite and CALJET aircraft observations of atmospheric rivers over the eastern North Pacific Ocean during the winter of 1997/98. *Mon. Wea. Rev.* **2004**, 132, 1721 –1745, doi: 10.1175/1520-0493(2004)132<1721:SACAOO>2.0.CO;2

13. Bao, J. W.; Michelson, S. A.; Neiman, P. J.; Ralph, F. M.; Wilczak, J. M. Interpretation of enhanced integrate d water vapor bands associated with extratropical cyclones: Their formation and connection to tropic al moisture. *Mon. Wea. Rev.* **2006**, 134, 1063–1080, doi: 10.1175/MWR3123.1

14. Neiman, P. J.; Ralph, F.M.; Wick, G.A.; Lundquist, J.D.; Dettinger, M.D. Meteorological characteristics and overland precipitation impacts of atmospheric rivers affecting the west coast of North America based on eight years of SSM/I satellite observations. *J. Hydrometeorol.* **2008**, 9, 22–47, doi: 10.1175/2007JHM855.1

15. Dacre, H.F.; Clark, P.A.; Martinez-Alvarado, O.; Stringer, M.A.; Lavers, D. A. How do atmospheric rivers form? *Bull. Am. Meteorol. Soc.* **2015**, 96, 1243–1255, doi: 10.1175/BAMS-D-14-00031.1

16. Gimeno, L.; Dominguez, F.; Nieto, R.; Trigo, R.; Drumond, A.; Reason, C. J.; Taschetto, A. S.; Ramos, A. M.; Kumar, R.; Jarengo, J. Major mechanisms of atmospheric moisture transport and their role in extreme precipitation events, *Annu. Rev. Env. Resour.* **2016**, 41, 117–141, doi: 10.1146/annurev-environ-110615-085558

17. Wernli, B. H.; Davies, H. C. A Lagrangian-based analysis of extratropical cyclones. I: The method and some applications. *Quart. J. Roy. Meteorol. Soc.* **1997**, 123(538), 467–489, doi: 10.1002/qj.49712353811.

18. Stohl, A.; James, P. A. Lagrangian analysis of the atmospheric branch of the global water cycle. Part I: Method description, validation, and demonstration for the August 2002 flooding in central Europe. *J. Hydrometeorol.* **2004**, 5, 656–678, doi: 10.1175/1525-7541(2004)005<0656:ALAOTA>2.0.CO;2

19. Hénin R.; Ramos A.M.; Pinto J.G.; Liberato L.R. A ranking of concurrent precipitation and wind events for the Iberian Peninsula. *Int J Climatol.* **2020**, 1 –17, doi: 10.1002/joc.6829

20. Eiras-Barca, J.; Lorenzo, N.; Taboada, J.; Robles, A.; MiguezMacho, G. On the relationship between atmospheric rivers, weather types and floods in Galicia (NW Spain). *Nat. Hazards Earth Syst. Sci.* **2018**, 18, 1633 –1645, doi: 10.5194/nhess-18-1633-2018.

21. Eiras-Barca, J.; Dominguez, F.; Hu, H.; Garaboa-Paz, D.; Miguez-Macho1, G. Evaluation of the moisture sources in two extreme landfalling atmospheric river events using an Eulerian WRF tracers tool. *Earth Syst. Dynam.* **2017**, 8, 1247–1261, doi: 10.5194/esd-8-1247-2017

22. Gimeno, L; Sthol, A.; Trigo, R.M.; Domínguez, F.; Yoshimura, K.; Yu, L.; Drumond, A.; Durán-Quesada, A.M.; Nieto, R. Oceanic and terrestrial sources of continental precipitation. *Rev. Geophys.* **2012**, 50, RG4003, doi: 10.1029/2012RG000389.

23. Nieto, R.; Gimeno, L.; Trigo, R. M. A Lagrangian identification of major sources of Sahel moisture. *Geophys. Res. Lett.* **2006**, 33, L18707, doi:10.1029/2006GL027232

24. Drumond, A.; Nieto, R.; Gimeno, L.; Ambrizzi, T. A Lagrangian identification of major sources of moisture over Central Brazil and La Plata Basin, *J. Geop hys. Res.* **2008**, 113, D14128, doi:10.1029/2007JD009547

25. Gimeno, L.; Drumond, A.; Nieto, R.; Trigo, R. M.; Stohl, A. On the origin of continental precipitation, *Geophys. Res. Lett.* **2010**, 37, L13804, doi:10.1029/2010GL043712

26. Durán-Quesada, A. M; Reboita, M. S.; Gimeno, L. (2012), Precipitation in tropical America and the associated sources of moisture: A short review. *Hydrol. Sci. J.* **2012**, 57, 612–624, doi: 10.1080/02626667.2012.673723

27. Gimeno, L.; Nieto, R.; Drumond, A.; Castillo, R.; Trigo, R. Influence of the intensification of the major oceanic moisture sources on continental precipitation. *Geophys. Res. Lett.* **2013**, 40, 1443–1450, doi:10.1002/grl.50338

28. Drumond, A.; Marengo, J.; Ambrizzi, T.; Nieto, R.; Moreira, L.; Gimeno, L. The role of the Amazon Basin moisture in the atmospheric branch of the hydrological cycle: A Lagrangian analysis. *Hydrol. Earth Syst. Sci.* **2014**, 18, 2577–2598, doi: 10.5194/hess-18-2577-2014

29. Ramos, A.M.; Nieto, R.; Tomé, R.; Gimeno, L.; Trigo, R. M.; Liberato, M. L. R.; Lavers, D. A. Atmospheric rivers moisture sources from a Lagrangian perspective. *Earth Syst. Dynam.* **2016**, 7, 371–384, doi: 10.5194/esd-7-371-2016

30. Gozzo, L.F; Rocha, R. P. da; Gimeno, L.; Drumond, A. Climatology and numerical case study of moisture sources associated with subtropical cyclogenesis over the southwestern Atlantic Ocean. *J. Geophys. Res.* **2017**, 122, 5636-5653, doi; 10.10022016JD025764

31. Ordoñez, P.; Nieto, R.; Gimeno, L.; Ribera, P.; Gallego, D.; Ochoa-Moya, C.A.; Quintanar, A.I. Climatological moisture sources for the Western North American Monsoon through a Lagrangian approach: their influence on precipitation intensity. *Earth Syst. Dynam.* **2019**, 10, 59-72, doi: 10.5194/esd-10-59-2019

32. Zhao, N.; Manda, A.; Guo. X.; Kikuchi, K.; Nasuno, T.; Nakano, M.; Zhang, Y.; Wang B. A Lagrangian View of Moisture Transport Related to the Heavy Rainfall of July 2020 in Japan: Importance of the Moistening Over the Subtropical Regions. *Geophys. Res. Lett.* **2021**, 48, e2020GL091441, doi: 10.10292020GL091441

33. Agencia Estatal de Meteorología. Available online: https://www.aemet.es/es/web/conocermas/borrascas/2018-2019/estudios_e_impactos/miguel (accessed on 12 March 2021).

34. Pinto, J.G.; Zacharias, S.; Fink, A.H. Factors contributing to the development of extreme North Atlantic cyclones and their relationship with the NAO. *Clim. Dyn.* **2009**, 32, 711 –737, doi: 10.1007/s00382-008-0396-4

35. Ulbrich, U.; Leckebusch, G.C.; Pinto, J.G. Extra-tropical cyclones in the present and future climate: a review. *THEOR. APPL CLIMATOL.* **2009**, 96, 117 –131, doi: 10.1007/s00704-008-0083-8

36. Raible, C.C.; Messmer, M.; Lehner, F.; Stocker, T.F.; Blender, R. Extratropical cyclone statistics during the last millennium and the 21st century. *Clim. Past* **2018**, 14, 1499 –1514, doi: 10.5194/cp-14-1499-2018.

37. Catto, J.L.; Ackerley, D.; Booth, J.; Champion, A.J.; Colle, A.B.; Pfahl, S.; Pinto, J.; Quinting, J.; Seiler, C. The future of mid-latitude cyclones. *Curr. Clim. Change Rep.* **2019**, 5, 407 –420, doi: 10.1007/s40641-019-00149-c4.

38. Naray A. Estudio de la excepcionalmente tardía e inusual ciclogénesis explosiva Miguel. Master Thesis. Universidad Complutense de Madrid. España Julio 13th 2020.

39. Hersbach, H.; Bell, B.; Berrisford, P.; Biavati, G.; Horányi, A.; Muñoz Sabater, J. et al. ERA5 hourly data on single levels from 1979 to present. Copernicus Climate Change Service (C3S) Climate Data Store (CDS) **2018**.

40. Dee, D. P. et al. The ERA-Interim reanalysis: Confiuration and performance of the data assimilation system. *Quart. J. Roy. Meteorol. Soc.* **2011**, 137, 553–597, doi: 10.1002/qj.828

41. Stohl, A.; Forster, C.; Frank, A.; Seibert, P.; Wotawa, G. Technical note: The Lagrangian particle dispersion model FLEXPART version 6.2, *Atmos. Chem. Phys.* **2005**, 5, 2461–2474, doi: 10.5194/acp-5-2461-2005

42. Blender, R.; Fraedrich, K.; Lunkeit, F. Identification of cyclone-track regimes in the North Atlantic. *Quart. J. Roy. Meteor. Soc.* **1997**, 123, 727–741

43. Peppler, A.; Dowdy, A. A Three-Dimensional Perspective on Extratropical Cyclone Impacts doi: 10.1175/JCLI-D-19-0445.1.

44. Sanders, F. and Gyakum, J. R. Synoptic-Dynamic Climatology of the "Bomb". *Mon. Wea. Rev.* **1980**, 108, 1589–1606, doi: 10.1175/1520-0493(1980)108<1589:SDCOT>2.0.CO;2

45. Numaguti, A. Origin and recycling processes of precipitating water over the Eurasian continent: Experiments using an atmospheric general circulation model. *J. Geophys. Res.* **1999**, 104, 1957–1972, doi: 10.1029/1998JD20002

46. Van der Ent, R. J.; Tuinenburg, O. A. The residence time of water in the atmosphere revisited, *Hydrol. Earth Syst. Sci.* **2017**, 21, 779–790, doi: 10.5194/hess-21-779-2017